



HAL
open science

Effect of electrode materials on the scaling behavior of energy density in $\text{Pb}(\text{Zr}_{0.96}\text{Ti}_{0.03})\text{Nb}_{0.01}\text{O}_3$ antiferroelectric films

J. Ge, G. Pan, Denis Remiens, Y. Chen, F. Cao, X.L. Dong, G.S. Wang

► **To cite this version:**

J. Ge, G. Pan, Denis Remiens, Y. Chen, F. Cao, et al.. Effect of electrode materials on the scaling behavior of energy density in $\text{Pb}(\text{Zr}_{0.96}\text{Ti}_{0.03})\text{Nb}_{0.01}\text{O}_3$ antiferroelectric films. Applied Physics Letters, 2012, 101, pp.112905-1-3. 10.1063/1.4752726 . hal-00788341

HAL Id: hal-00788341

<https://hal.science/hal-00788341>

Submitted on 27 May 2022

HAL is a multi-disciplinary open access archive for the deposit and dissemination of scientific research documents, whether they are published or not. The documents may come from teaching and research institutions in France or abroad, or from public or private research centers.

L'archive ouverte pluridisciplinaire **HAL**, est destinée au dépôt et à la diffusion de documents scientifiques de niveau recherche, publiés ou non, émanant des établissements d'enseignement et de recherche français ou étrangers, des laboratoires publics ou privés.

Effect of electrode materials on the scaling behavior of energy density in $\text{Pb}(\text{Zr}_{0.96}\text{Ti}_{0.03})\text{Nb}_{0.01}\text{O}_3$ antiferroelectric films

Cite as: Appl. Phys. Lett. **101**, 112905 (2012); <https://doi.org/10.1063/1.4752726>

Submitted: 29 June 2012 • Accepted: 31 August 2012 • Published Online: 14 September 2012

Jun Ge, Gang Pan, Denis Remiens, et al.



View Online



Export Citation

ARTICLES YOU MAY BE INTERESTED IN

Enhanced polarization switching and energy storage properties of $\text{Pb}_{0.97}\text{La}_{0.02}(\text{Zr}_{0.95}\text{Ti}_{0.05})\text{O}_3$ antiferroelectric thin films with LaNiO_3 oxide top electrodes

Applied Physics Letters **102**, 142905 (2013); <https://doi.org/10.1063/1.4801517>

Effect of residual stress on energy storage property in PbZrO_3 antiferroelectric thin films with different orientations

Applied Physics Letters **103**, 162903 (2013); <https://doi.org/10.1063/1.4825336>

Composition-dependent dielectric and energy-storage properties of $(\text{Pb},\text{La})(\text{Zr},\text{Sn},\text{Ti})\text{O}_3$ antiferroelectric thick films

Applied Physics Letters **102**, 163903 (2013); <https://doi.org/10.1063/1.4802794>

Lock-in Amplifiers
up to 600 MHz



Zurich
Instruments



Effect of electrode materials on the scaling behavior of energy density in $\text{Pb}(\text{Zr}_{0.96}\text{Ti}_{0.03})\text{Nb}_{0.01}\text{O}_3$ antiferroelectric films

Jun Ge,¹ Gang Pan,¹ Denis Remiens,² Ying Chen,¹ Fei Cao,¹ Xianlin Dong,¹ and Genshui Wang^{1,a)}

¹Key Laboratory of Inorganic Functional Materials and Devices, Shanghai Institute of Ceramics, Chinese Academy of Sciences, 1295 Dingxi Road, Shanghai 200050, People's Republic of China

²IEMN-DOAE, CNRS UMR 8520, Cité scientifique, 59655 Villeneuve-d'Ascq Cedex, France

(Received 29 June 2012; accepted 31 August 2012; published online 14 September 2012)

Antiferroelectric $\text{Pb}(\text{Zr}, \text{Nb}, \text{Ti})\text{O}_3$ (PZNT) films were deposited via a sol-gel process on Pt(111)/Ti/SiO₂/Si, LaNiO₃- and La_{0.5}Sr_{0.5}CoO₃-buffered Si substrate. The scaling behavior of the energy density W of antiferroelectric films was investigated. The scaling behavior of W against frequency f of PZNT on LaNiO₃-buffered Si takes the form of $W \propto f^{0.08}$, which differs significantly from that form of $W \propto f^{-0.14}$ of PZNT on La_{0.5}Sr_{0.5}CoO₃-buffered Si. This indicates that the scaling relations of W vary substantially as bottom electrodes change and might be closely related to the variation of nonuniform strain field and depolarization field within the AFE films. © 2012 American Institute of Physics. [<http://dx.doi.org/10.1063/1.4752726>]

Antiferroelectric (AFE) materials are promising candidates of great current interest for future high-energy and fast-speed storage capacitors.^{1,2} Thin films of AFE and ferroelectric (FE) materials are of particular interest due to their relevant applications in connection with microelectronic devices. It was reported that a remarkable energy density as high as 14.9 J/cm³ at 600 kV/cm was obtained in La-modified PbZrO₃ thin films.³ Recently, A very large energy storage density up to 13.7 J/cm³ was also exhibited by eliminating a secondary pyrochlore phase in PbZrO₃-based AFE films.⁴ On the other hand, devices in practical applications are often required to operate under conditions of varying frequencies and electric fields, therefore, the scaling behavior of W , i.e., W as a function of the field amplitude E_0 and frequency f , has become an important consideration.⁵⁻⁷ Though there are several reports about scaling relation of W against E_0 on doped PbZrO₃ (PZ) AFE films,^{3,4} the scaling behavior of W against f and the effect of bottom electrode materials in PZ AFE films have not yet been studied. In this letter, LaNiO₃ (LNO), Pt, and La_{0.5}Sr_{0.5}CoO₃ (LSCO) were employed as bottom electrodes on Si substrate for growing $\text{Pb}(\text{Zr}_{0.96}\text{Ti}_{0.03})\text{Nb}_{0.01}\text{O}_3$ (PZNT) AFE films which are close to the AFE-FE phase boundary in the PZT ternary system, and their structure, switching, and scaling behavior have been investigated.

The capacitors were fabricated by chemical solution deposition. PZNT films deposited on the LNO/SiO₂/Si denoted as S1 and the Pt/Ti/SiO₂/Si-S2 and the LSCO/SiO₂/Si-S3, respectively. The precursor solution for LNO and LSCO was prepared from La acetate, Sr acetate, Ni acetate, and Co acetate. The LNO, LSCO, and Pt layers all have thickness of about 150 nm. The precursor solution for PZNT was prepared from Pb acetate, Zr propoxide, Ti isopropoxide, and Ni ethoxide. In order to compensate the lead loss during annealing and prevent the formation of a pyrochlore phase, 10 mol. % excess of lead acetate trihydrate was added, and films were prepared through a multiple layer spin-

coating procedure. Each spun-on PZNT layer was heated at 650 °C for 5 min. The spin coating and heat treatment were repeated several times to obtain the desired thickness. The structure and phase purity of the films were checked using x-ray diffractometry (XRD) in a θ - 2θ scan. The electrical measurements were carried out on capacitor structures fabricated with Pt top electrode (diameter of $\sim 250 \mu\text{m}$) sputtered through a photolithography process. The surface morphologies and phase microstructure were observed using scanning electron microscope. The dielectric and ferroelectric properties were measured using a broadband dielectric spectrometer and a ferroelectric tester.

Figure 1 shows three typical XRD patterns of the PZNT film S1, S2, and S3. It can be observed that all films displayed a pure perovskite structure and no impurity phase is found. For film S3, the pure phase has no obvious preferred orientation. In contrast, film S1 shows highly oriented (100) fiber texture and film S2 shows (111) fiber texture. It is apparent that LNO forms a template facilitating grain-on-grain growth of the overlaying PZNT films.⁸ As for film S2, the proposed nucleation mechanism was the formation of a (111)-oriented transient intermetallic phase, such as Pt₃Ti or Pt₃Pb, at the interface of films and Pt electrodes.⁹ Hence, the deposited films were induced to grow along the (111)-orientation. Cross-section SEM image of film S1 is shown as an inset in Figure 1. The SEM images of S2 and S3 which are not shown here are similar to those of S1. All films exhibit a dense microstructure with a thickness of about 1 μm . Clear columnar structure can be found in cross-section images. This indicates that the perovskite grains nucleate at the film-electrode interface and grow through the film to the free surface, as reported in PZT thin films.¹⁰

Figure 2 shows a group of dynamic hysteresis (P-E) loops and scaling relation of W against f of PZNT films grown on different substrates. Data were taken at different frequencies from 20 to 1000 Hz (some hysteresis loops not shown here) and the applied ac electric field was kept at 500 kV/cm. All films have double hysteresis loops indicating the AFE nature and some remanent polarization which is

^{a)}Electronic mail: genshuiwang@mail.sic.ac.cn.

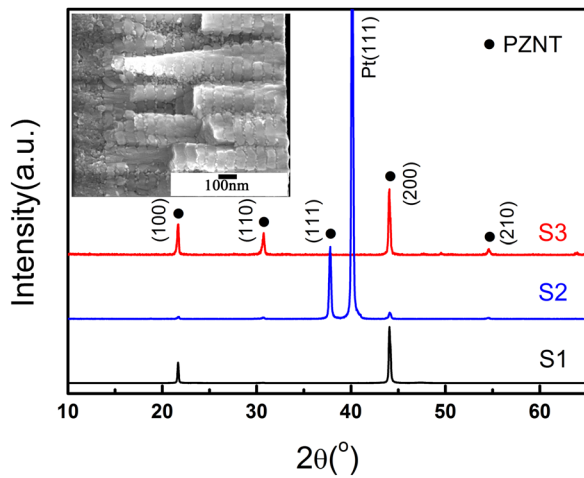


FIG. 1. Room temperature XRD θ - 2θ of films S1-S3 grown on different substrates. The inset shows the microstructure of the cross-section of the PZNT/LNO/Si films.

believed to be due to the retention of ferroelectric phase after field removal.¹¹ Whereas the P-E loops are measured for films with different bottom electrodes, the FE-AFE back switching field tends to decrease as the samples change from S1 to S3. In general, the FE-AFE back switching time decreases with increasing value of back switching field.² Hence, These behaviors may demonstrate that the FE-AFE phase switching time of film S3 is longer than that of other samples. As frequency varies, the films S1 and S2 display a frequency-dependent hysteresis loops with both of their P_S (saturated polarization) and P_r (remanent polarization) decrease a little as the frequency increases. Surprisingly, hysteresis loops of S3 demonstrate a much different frequency-dependent relationship. With increasing the frequency from 50 to 200Hz, the P_r increased dramatically from $\sim 8.6 \mu\text{C}/\text{cm}^2$ to $\sim 15.7 \mu\text{C}/\text{cm}^2$. Enlightened from the scaling relations in a Nb-doped lead zirconate titanate stan-

nate (PZST) AFE bulk ceramic,⁷ we fit these data of double loops with $W \propto f^\alpha$ to obtain the suitable scaling relations of PZNT films. The f-term exponent α is obtained by plotting $\log W$ against $\log f$ at fixed E. As plotted in Fig. 2(d), it is revealed that for film S1, α is 0.08 which means W increases gradually with frequency increases. However, the W of film S2 is basically remains unchanged ranging from 20 to 1000 Hz. As for film S3, W decreases rapidly with varying frequency as α is -0.14 . We believe that the different response behaviors of W - f curves may be attributed to the different amount of retained FE phase in film S1 to S3. As we mentioned before, the FE-AFE phase switching speed is slower in film S3 because of the lower FE-AFE switching field, hence at high frequencies, the FE-AFE phase switching time of film S3 may be comparable with the switching time for “single shot” hysteresis measurements, thus, some of the ferroelectric domains may be retained beyond the transformation from the FE to the AFE state, which results the remanent polarization increase and W decrease of film S3. Interestingly, a previous investigation¹² on $0.89\text{Ba}_{0.5}\text{Na}_{0.5}\text{TiO}_3-0.06\text{BaTiO}_3-0.05\text{K}_{0.5}\text{Na}_{0.5}\text{NbO}_3$ (BNT-BT-KNN) AFE ceramics yielded scaling behaviors very similar to those of our films. In that case W is basically independent of frequency at 383 K for major AFE phases, and the ceramics transform into a mixture of AFE and FE phases when subject to a relatively low temperature at 293 K, where W decreases from 0.51 to $0.44 \text{ J}/\text{cm}^3$ with increasing frequency from 1 to 100 Hz.

The dependence curves of W on E_0 observed at 100 Hz shown in Fig. 3 were investigated. For film S1, the W - E_0 curves are similar to those in typical AFE PNZST ceramics⁷ and La-modified PbZrO_3 thin films.⁴ The change of the curves follows a step-like function and when the electric fields approach E_{AF} (AFE-FE switching field), the energy densities rise steeply from 0.96 to $3.49 \text{ J}/\text{cm}^3$ with increasing of E_0 from 300 to 400 kV/cm. On the other hand, film S2 shows a little diffused curve and the energy density at

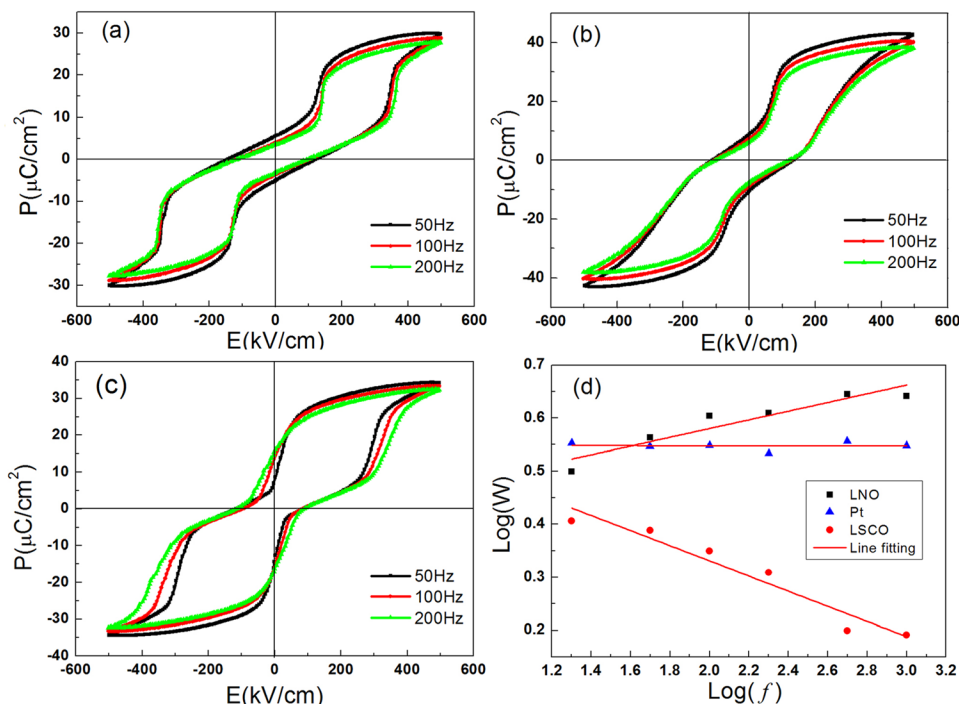


FIG. 2. Scaling of hysteresis for PZNT films on different substrates: variation in hysteresis loops of AFE films (a) PZNT/LNO/Si films, respectively (S1), (b) PZNT/Pt/Si (S2), (c) PZNT/LSCO/Si (S3), as a function of frequency. (d) The relation of $\log(W)$ against $\log(f)$ for the saturated hysteresis loops.

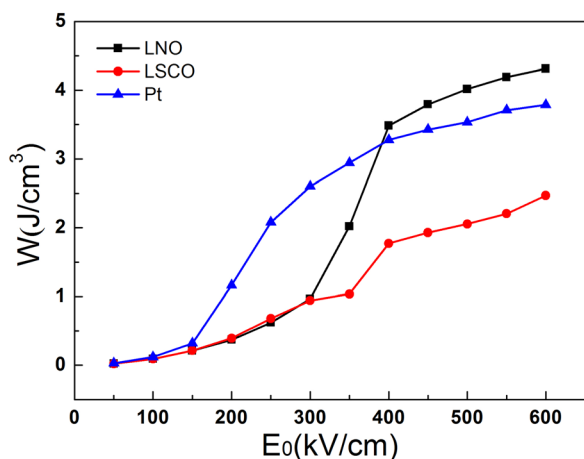


FIG. 3. Dependence of energy density W on field amplitude E_0 at 100 Hz.

400 kV/cm is 3.28 J/cm³ which is little less than that of film S1. This could be explained by the increase of stable retained FE state in film grown on Pt/SiO₂/Si. Especially, for film S3, the energy density shows a much more diffused curve with only a little jump from 0.94 to 1.77 J/cm³ at between 300 and 400 kV/cm, which is very similar to that of soft Nb-doped ferroelectric Pb(Zr_{0.52}Ti_{0.48})O₃ ceramics.¹³ The results indicate a much more percentage of stable FE phase retention in PZNT films on LSCO/SiO₂/Si, which further prove the result we discussed before.

The coexistence of ferroelectricity and antiferroelectricity in films has been explained by the lattice strain¹⁴ or surface charges and self-biasing¹⁵ at the interfaces between the films and substrates. However, these interpretations seem not to work for our films because they all based on a precondition that the films should be at least thinner than 300 nm. Here, we believe there are two major factors influencing the results in our cases. The first one is related to the nonuniform strain field.¹⁶ When the grains in films deform because of polarization switching under the applied electric field, each grain containing AFE/FE domains experiences a strain field, depending on the orientation of adjacent grains and configuration of domains therein. As we mentioned before, film S3 is less oriented than film S1 and S2, so one can expect to see more nonuniform strain field of film S3 than that of film S1 and S2. The result is that in some regions of film S3, the strain field is large enough that the field-induced FE phase may no longer be able to switch back, therefore, giving rise to the relatively larger remanent polarization. The second potential cause is related to the depolarization field generated during polarization. Normally the depolarization field substantially affects the physical properties of ferroelectrics, because this field tends to suppress spontaneous polarization and, thus, to destroy the ferroelectric state. However, the depolarization field may help the FE phases return back to AFE phases in antiferroelectric. Electrode can considerably decrease the depolarization field.¹⁷ For example, superconducting electrodes in bulk ferroelectrics lead to complete

compensation for the depolarization field.^{17,18} The PZNT films can be treated as a p-type semiconductor because of the unavoidable Pb vacancies,¹⁹ so at the PZT/LNO and PZT/LSCO interfaces, p-n-like^{20,21} and p-p-like junctions will be formed.²² However, the barrier height in the p-p junction is usually lower,¹⁹ whereas the barrier height in the p-n junction should be larger and compensation for the depolarization field is difficult resulting in easier returning back to AFE phases at low electric field and smaller remanent polarization.

In summary, energy-storage properties and scaling behavior of Pb(Zr_{0.96}Ti_{0.03})Nb_{0.01}O₃ films using different bottom electrodes were first investigated. Although with similar composition and thickness, the scaling relation for energy densities of films on LNO/SiO₂/Si takes the form of $W \propto f^{0.08}$, which is very different from $W \propto f^{-0.14}$ of films on LSCO/SiO₂/Si. Additionally, the scaling relation of films on Pt/Ti/SiO₂/Si shows that W is basically independent of frequency. These behaviors demonstrate that electrode materials might heavily influence the scaling behavior of energy density in Pb(Zr_{0.96}Ti_{0.03})Nb_{0.01}O₃ antiferroelectric films, which is closely related to the nonuniform strain field and depolarization field generated within the AFE films.

¹B. M. Xu, P. Moses, N. G. Pal, and L. E. Cross, *Appl. Phys. Lett.* **72**(5), 593 (1998).

²W. Y. Pan, C. Q. Dam, Q. M. Zhang, and L. E. Cross, *J. Appl. Phys.* **66**(12), 6014 (1989).

³J. Parui and S. B. Krupanidhi, *Appl. Phys. Lett.* **92**(19), 192901 (2008).

⁴M. S. Mirshekarloo, K. Yao, and T. Sritharan, *Appl. Phys. Lett.* **97**(14), 142902 (2010).

⁵Y. W. So, D. J. Kim, T. W. Noh, J. G. Yoon, and T. K. Song, *Appl. Phys. Lett.* **86**(9), 092905 (2005).

⁶R. Yimnirun, Y. Laosiritaworn, S. Wongsanmai, and S. Ananta, *Appl. Phys. Lett.* **89**(16), 162901 (2006).

⁷X. Chen, F. Cao, H. Zhang, G. Yu, G. Wang, X. Dong, Y. Gu, H. He, and Y. Liu, *J. Am. Ceram. Soc.* **95**(4), 1163 (2012).

⁸J. W. Zhai, M. H. Cheung, K. X. Zheng, L. Xin, H. D. Chen, E. V. Colla, and T. B. Wu, *Appl. Phys. Lett.* **81**(19), 3621 (2002).

⁹J. W. Li, H. Kameda, B. N. Q. Trinh, T. Miyasako, P. T. Tue, E. Tokumitsu, T. Mitani, and T. Shimoda, *Appl. Phys. Lett.* **97**(10), 102905 (2010).

¹⁰M. J. Lefevre, J. S. Speck, R. W. Schwartz, D. Dimos, and S. J. Lockwood, *J. Mater. Res.* **11**(8), 2076 (1996).

¹¹S. S. Sengupta, D. Roberts, J. F. Li, M. C. Kim, and D. A. Payne, *J. Appl. Phys.* **78**(2), 1171 (1995).

¹²F. Gao, X. L. Dong, C. L. Mao, W. Liu, H. L. Zhang, L. H. Yang, F. Cao, and G. S. Wang, *J. Am. Ceram. Soc.* **94**(12), 4382 (2011).

¹³X. F. Chen, X. L. Dong, H. L. Zhang, G. Yu, F. Cao, and G. S. Wang, *Solid State Commun.* **150**(15-16), 720 (2010).

¹⁴A. R. Chaudhuri, M. Arredondo, A. Hahnel, A. Morelli, M. Becker, M. Alexe, and I. Vrejoiu, *Phys. Rev. B* **84**(5), 054112 (2011).

¹⁵P. Ayyub, S. Chattopadhyay, R. Pinto, and M. S. Multani, *Phys. Rev. B* **57**(10), R5559 (1998).

¹⁶J. W. Zhai and H. D. Chen, *Appl. Phys. Lett.* **83**(5), 978 (2003).

¹⁷M. D. Glinchuk, B. Y. Zaulychny, and V. A. Stephanovich, *Phys. Solid State* **47**(7), 1331 (2005).

¹⁸M. D. Glinchuk, B. Y. Zaulychny, and V. A. Stephanovich, *Ferroelectrics* **316**, 1 (2005).

¹⁹F. Chen, Q. Z. Liu, H. F. Wang, F. H. Zhang, and W. B. Wu, *Appl. Phys. Lett.* **90**(19), 192907 (2007).

²⁰A. Wold, B. Post, and E. Banks, *J. Am. Chem. Soc.* **79**(18), 4911 (1957).

²¹K. P. Rajeev, G. V. Shivashankar, and A. K. Raychaudhuri, *Solid State Commun.* **79**(7), 591 (1991).

²²Y. Watanabe, *Phys. Rev. B* **59**(17), 11257 (1999).